Title

Aqueous RAFT at pH zero: enabling controlled polymerization of unprotected acyl hydrazide methacrylamides

Journal

Polymer Chemistry, 8(34)

ISSN

1759-9954

Authors

Hoff, Emily A
Abel, Brooks A
Tretbar, Chase A
et al.

Publication Date

2017

DOI

10.1039/c6py01563h

Peer reviewed

Volume 8 | Number 34 | 14 September 2017 | Pages 4891–5254

Polymer Chemistry

rsc.li/polymers

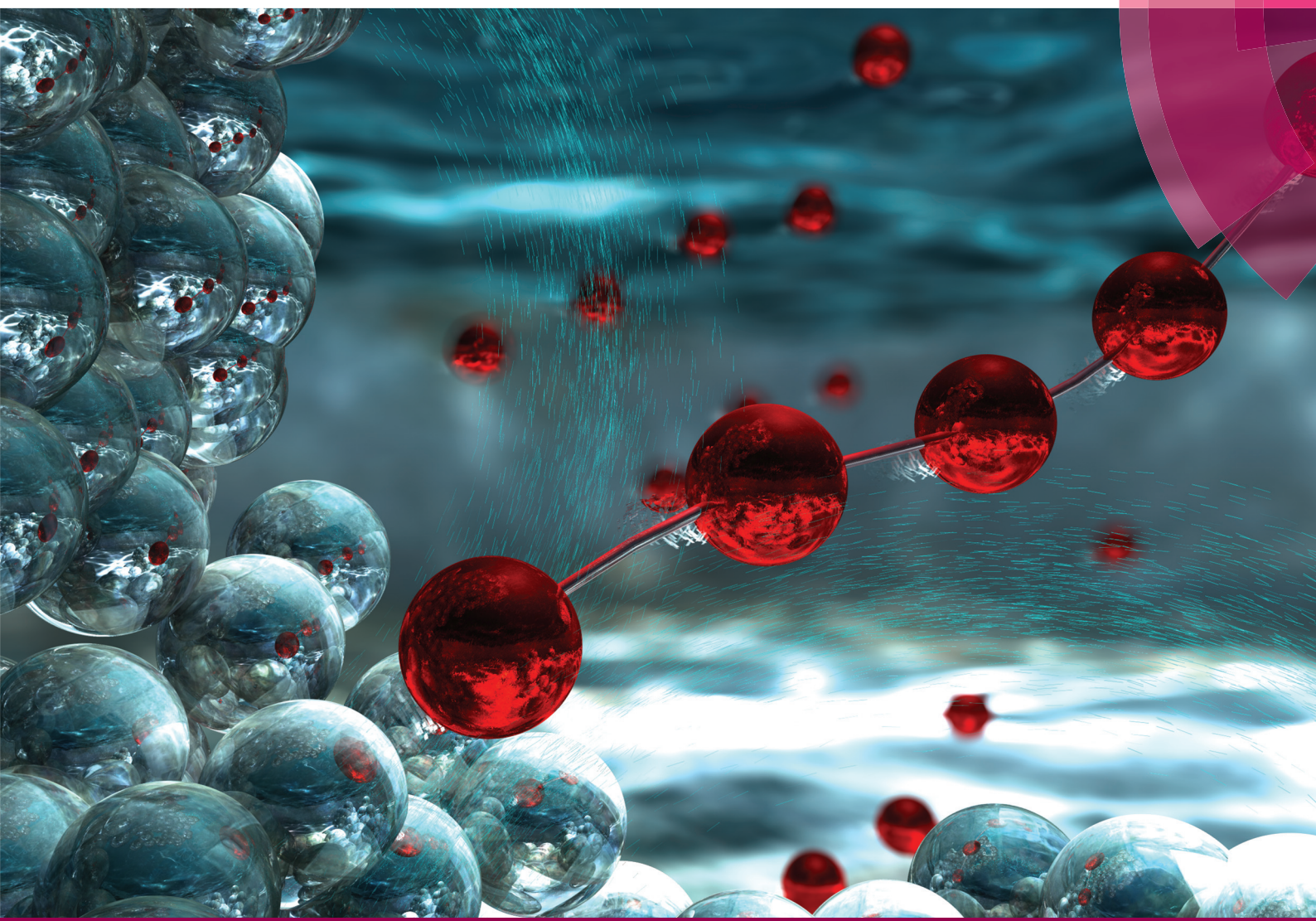

Themed issue: Pioneering Investigators 2017

ISSN 1759-9962

ROYAL SOCIETY OF CHEMISTRY

COMMUNICATION
Derek L. Patton *et al.*
Aqueous RAFT at pH zero: enabling controlled polymerization of unprotected acyl hydrazide methacrylamides

Polymer Chemistry

COMMUNICATION

View Article Online
View Journal | View Issue

Cite this: *Polym. Chem.*, 2017, **8**, 4978

Received 6th September 2016,
Accepted 15th October 2016

DOI: 10.1039/c6py01563h

rsc.li/polymers

Aqueous RAFT at pH zero: enabling controlled polymerization of unprotected acyl hydrazide methacrylamides†

Emily A. Hoff, Brooks A. Abel, Chase A. Tretbar, Charles L. McCormick and Derek L. Patton*

We report aqueous RAFT polymerization at pH = 0 mediated by a novel imidazolium-containing chain transfer agent. In 1 M HCl, unprecedented controlled polymerization and chain-extension of unprotected acyl hydrazide methacrylamides is achieved enabling the synthesis of well-defined acyl hydrazide functionalized polymer scaffolds of interest for dynamic covalent and bioconjugation strategies.

Acyl hydrazides are potent functional groups for C=N bond formation and exchange reactions with active carbonyl compounds yielding pH responsive hydrazones (Scheme 1a) and represent one of the most widely employed dynamic covalent chemical handles.[1–4] Efforts have recently increased to precisely install these functional groups in polymer scaffolds for applications such as bioconjugation/controlled release,[5–10] supramolecular and coordination motifs,[4] dynamic nanoparticles,[11] stimuli-responsive actuation,[12] and network formation.[13–16] The chemical attributes of acyl hydrazides (*e.g.*, high nucleophilicity, low pK_a, and metal coordination affinity) present a synthetic challenge for controlled polymerization techniques. Consequently, acyl hydrazides are most often installed on well-defined polymer scaffolds by polymerization of protected monomers (*e.g.* BOC-protected,[9] acetoxime-protected[10]) or *via* postpolymerization modification (PPM) techniques (*e.g.* hydrazinolysis of ester pendent groups).[15,17] These synthetic approaches are broadly employed to achieve hydrazide-functionalized polymers but often require multistep PPM reactions and purifications, or the undesired use of hydrazine (anhydrous or hydrate form) as a chemical reagent. Alternatively, hydrazide-functionalized polymers have been obtained *via* conventional free radical polymerization of unprotected methacryloyl hydrazide (or similar derivatives);[5,6,8] however, this approach does not provide access to hydrazide-functionalized polymer scaffolds with well-defined molecular weights and/or complex macromolecular architectures.

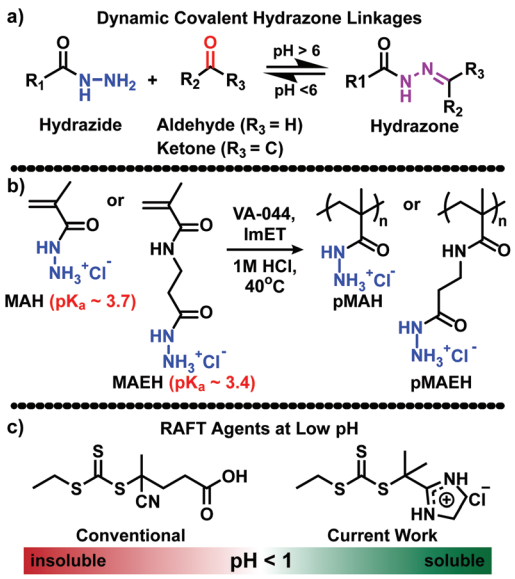

Scheme 1 (a) Dynamic covalent hydrazone equilibrium, (b) aRAFT polymerization of acyl hydrazide monomers with low pK_a values and (c) general chain transfer agent structure and R-groups at low pH.

Reversible addition–fragmentation chain transfer (RAFT) polymerization has made possible the synthesis of functional polymers with controlled molecular weights, low dispersities and complex architectures, and offers excellent utility for the controlled polymerization of monomers bearing strongly nucleophilic functional groups.[18–21] In particular, aqueous RAFT (aRAFT) has enabled the direct polymerization of amide- or amine-containing monomers (pK_a values ≈9) by employing pH 5 buffer solutions as the polymerization medium – conditions that protonate the nucleophilic sites and suppress aminolysis of thiocarbonylthio-based chain transfer agents (CTAs).[22–26] Meanwhile, aRAFT polymerizations of nucleophilic monomers with pK_a values <7 require substantially more acidic polymerization conditions to prevent CTA aminolysis.

School of Polymers and High Performance Materials. The University of Southern Mississippi, Hattiesburg, MS 39406, USA. E-mail: derek.patton@usm.edu

†Electronic supplementary information (ESI) available: Experimental details, NMR spectra. See DOI: 10.1039/c6py01563h

For example, Allen *et al.*[27] recently attempted aRAFT of 4-vinylimidazole ($pK_a \approx 6$) in pH 5.2 acetate buffer with limited success, but found polymerizations conducted in glacial acetic acid ($pK_a = 4.76$) afforded excellent control over MW and dispersity. Monomers containing unprotected acyl hydrazides exhibit pK_a values <4, and would therefore require a polymerization medium with significantly lower pH (*e.g.* <1) to ensure near quantitative protonation of the nucleophilic hydrazides.

To our knowledge, controlled polymerization of unprotected acyl hydrazide monomers has not been reported. In this work, we demonstrate the unprecedented controlled aRAFT polymerization of unprotected acyl hydrazide functionalized monomers under low pH conditions (pH = 0). A new imidazolium-functionalized CTA was synthesized to promote solubility at low pH and to afford excellent polymerization control using 1 M HCl. The polymerizations of two methacrylamide monomers, methacryloyl hydrazide hydrochloride (MAH) and (2-methacrylamidoethyl) carbohydrazide hydrochloride (MAEH), were explored. The ethyl spacer in the latter proved to be especially important to achieve living chain-end retention (*vide infra*). Successful chain extension of a p(MAEH) macro-CTA provided additional evidence of high trithiocarbonate end group retention and further highlighted the extent of polymerization control. Notably, the current work enables the synthesis of well-defined hydrazide-functionalized polymer scaffolds with complex architectures without requiring protection chemistry or postpolymerization modification.

Results and discussion

To demonstrate the utility of low pH aRAFT polymerization to provide well-defined polymers from unprotected acyl hydrazide monomers, we prepared representative monomers, methacryloyl hydrazide hydrochloride (MAH) and (2-methacrylamidoethyl) carbohydrazide hydrochloride (MAEH) (Scheme 1b), according to procedures reported in the ESI.† The pK_a values of MAH and MAEH were then measured by potentiometric titration to be 3.70 and 3.43, respectively (Table S1†). It should be noted, these values are substantially lower than the pK_a values for primary amine-containing monomers ($pK_a \approx 9$) that have been previously polymerized in acetate buffer (pH = 5.0) using aRAFT,[18,25] and thus a more acidic polymerization medium is required to ensure acyl hydrazide protonation. Based on the pK_a values of MAH and MAEH, an aqueous solvent with pH = 0 is necessary to ensure >99.9% monomer acyl hydrazide protonation.

With this in mind, 1 M HCl (aq) was selected as the polymerization solvent and a new CTA was designed to provide both solubility and hydrolytic stability at this low pH value. When compared to dithiobenzoate CTAs, trithiocarbonates generally exhibit slower rates of hydrolysis[28] and promote higher polymerization rates while maintaining polymerization control.[29] For example, Baussard and coworkers reported that trithiocarbonate CTAs were hydrolytically stable at pH = 1–2 when endowed with appropriate functionality for solubility (*e.g.*, sulfonate, quaternary amine) while traditional CTAs with carboxylic acid R-groups were not soluble in this pH range (Scheme 1c).[23] Taking these factors into consideration, we synthesized in a relatively high overall yield (65%), 2-(ethylthiocarbonothioylthio) 2-(2-imidazolin-2-yl)propane hydrochloride (ImET) – a trithiocarbonate CTA containing an imidazolium R-group selected based on its solubility at low pH and resemblance to the low temperature initiator VA-044 used in subsequent polymerizations (Scheme 1c).

First, MAH was polymerized in 1 M HCl (pH = 0) using ImET as the CTA and VA-044 as the low decomposition temperature initiator at $[M]_0:[CTA]_0:[I]_0 = 250:1:0.25$. Fig. 1a shows the kinetic plot for the polymerization at 40 °C. Following a 60 min initialization period, linear pseudo-first-order kinetic behavior was observed up to 600 min. Initialization behavior, as described by Klumperman and coworkers,[30] is most likely attributed to slow fragmentation and reinitiation of and by the CTA R-group. Aqueous size exclusion chromatography (ASEC) analysis of ImET-mediated aRAFT polymerization of MAH yielded chromatograms exhibiting low molecular weight tailing (Fig. 1b) and high dispersities that increase with conversion ($Đ_M$ = 1.22–1.31). Furthermore, while Fig. 1c shows a linear increase in M_{nexp} *vs.* monomer conversion as determined by ASEC-MALLS, the M_{nexp} values are higher than theoretically predicted based upon monomer conversion and a 250 : 1 $[M]_0:[CTA]_0$ ratio. A loss in yellow color was also observed after prolonged reaction times and is suggestive of trithiocarbonate degradation *via* hydrolysis or aminolysis during MAH polymerization in 1 M HCl – a process that would yield low MW tailing resulting from a reduced number of "living" chain ends.[24] This outcome is surprising,

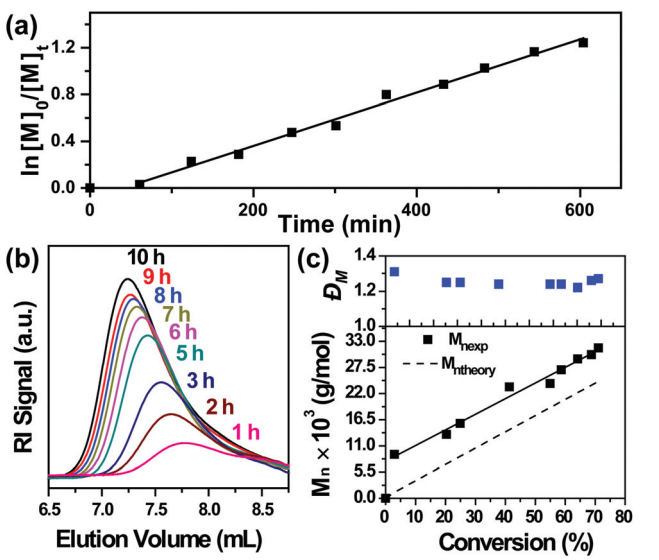

Fig. 1 (a) ASEC traces for polymerization kinetics of MAH, (b) dispersities and M_n *vs.* conversion plot, and (c) pseudo-first order kinetic plot for aRAFT polymerization of MAH in 1 M HCl with VA-044 and ImET at 40 °C.

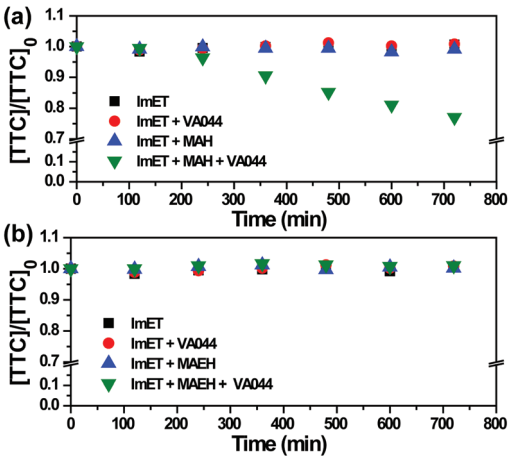

Fig. 2 (a) Degradation kinetics of ImET in 1 M HCl (black ■) and in the presence of initiator (red ●), MAH (blue ▲), and initiator plus MAH (green ▼) at $[M]_0 : [ImET]_0 : [VA\text{-}044]_0 = 10 : 1 : 0.2$ and 40 °C under argon. (b) Degradation kinetics of ImET in 1 M HCl (black ■) and in the presence of initiator (red ●), MAEH (blue ▲), and initiator plus MAEH (green ▼) at $[M]_0 : [ImET]_0 : [VA\text{-}044]_0 = 10 : 1 : 0.2$ and 40 °C under argon.

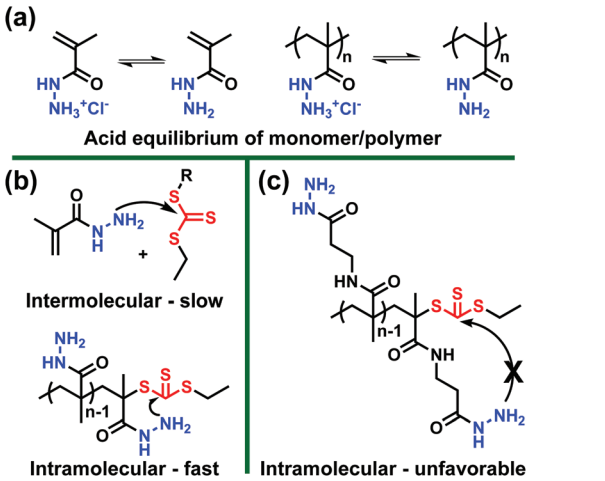

Scheme 2 (a) Acid equilibrium of MAH monomer and polymer, (b) proposed mechanisms for inter- and intramolecular monomer-induced trithiocarbonate chain-end degradation, (c) unfavorable intramolecular aminolysis *via* MAEH.

however, since the number of unprotonated hydrazide groups capable of aminolysis should be insignificant at pH ≈ 0.

We next sought to elucidate the exact cause of trithiocarbonate (TTC) chain-end degradation during the ImET-mediated polymerization of MAH in 1 M HCl by investigating the individual and combined influences of solvent, monomer, and initiator on the fractional change in trithiocarbonate concentration ($[TTC]/[TTC]_0$) at 40 °C as measured by UV-Vis spectroscopy (λ = 315 nm). Fig. 2a reveals no measurable independent influences of 1 M HCl (black ■), VA-044 (red ●), or MAH (blue ▲) on $[TTC]/[TTC]_0$ at 40 °C. This result suggests that ImET is stable towards hydrolysis at low pH and that the hydrazide functional groups of MAH are protonated sufficiently to prevent intermolecular aminolysis of the CTA. However, when ImET, MAH, and VA-044 were combined at 40 °C in 1 M HCl such that polymerization occurs (Fig. 2a, green ▼), a 25% decrease in $[TTC]/[TTC]_0$ is observed after 720 min. This result shows that trithiocarbonate chain-end degradation only takes place during polymerization and is indeed the cause of poor molecular weight control during the ImET-mediated polymerization of MAH in 1 M HCl. Because trithiocarbonate degradation was only observed following the covalent addition of monomer to CTA (*i.e.* during polymerization), we hypothesized that intramolecular attack of the trithiocarbonate chain-end by the hydrazide group of the ultimate monomer unit is likely responsible for the decrease in $[TTC]/[TTC]_0$ measured during polymerization of MAH at 40 °C as illustrated in Scheme 2b. At pH = 0, the acid equilibrium (Scheme 2a) is shifted in favor of protonated acyl hydrazide functional groups; however, when transient deprotonation of the terminal acyl hydrazide occurs, the ultimate MAH unit can adopt a favorable conformation to react with the thiocarbonyl of the terminal trithiocarbonate six atoms away with much higher collision frequency than the analogous intermolecular reaction (Scheme 2b). Similarly, Abel and coworkers recently demonstrated that CTA degradation during the RAFT polymerization of *N*-arylmethacrylamides occurs by intramolecular nucleophilic attack of the terminal trithiocarbonate by the ultimate methacrylamide monomer unit.[31]

To address the issue of trithiocarbonate chain-end degradation, we synthesized MAEH, an analogue of MAH that positions the acyl hydrazide further from the methacrylamide backbone (Scheme S1c†). As shown in Scheme 2c, intramolecular nucleophilic attack of the trithiocarbonate chain-end by the acyl hydrazide group of the ultimate MAEH unit is unlikely due to the unfavorable formation of a 10 atom cyclic product. The influence of MAEH on trithiocarbonate degradation during polymerization was investigated using UV-Vis spectroscopy. The $[TTC]/[TTC]_0$ *vs.* time for ImET at 40 °C in 1 M HCl with VA-044, MAEH, and ImET plus MAEH and VA-044 are shown in Fig. 2b. Trithiocarbonate degradation was not observed under the conditions representative of MAEH polymerization (Fig. 2b, green ▼). This result supports the hypothesis that trithiocarbonate chain-end degradation during the polymerization of MAH is due to intramolecular attack by the terminal monomer unit on trithiocarbonate and that adding an ethyl spacer between methacrylamide and acyl hydrazide functional groups places the terminal hydrazide group in an unfavorable position to react with CTA.

After illuminating the cause of CTA degradation, MAEH was polymerized at 40 °C in 1 M HCl with VA-044 as the initiator using a $[M]_0 : [CTA]_0 : [I]_0 = 250 : 1 : 0.20$. In contrast to aRAFT polymerization of MAH, well-controlled polymerization behavior of MAEH was achieved. The ASEC RI traces shown in Fig. 3b are narrow, symmetrical, and shift to lower elution volumes with polymerization time without low molecular weight tailing. Dispersities, shown in Fig. 3c, also remain low

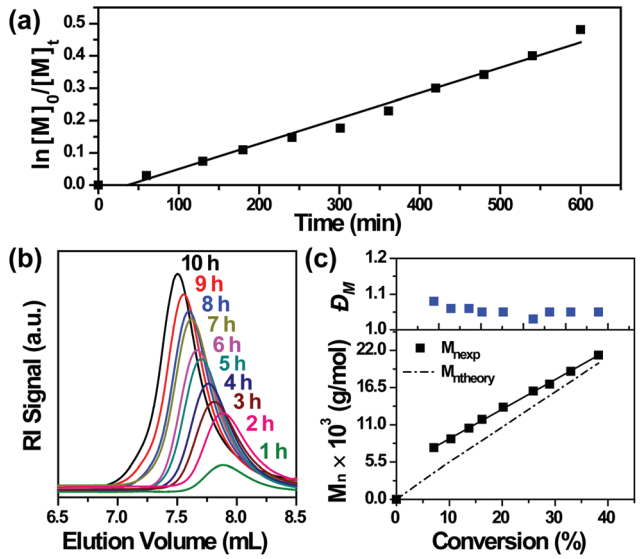

Fig. 3 (a) ASEC traces for polymerization kinetics of MAEH, (b) dispersities and M_n *vs.* conversion plot, and (c) pseudo-first order kinetic plot for aRAFT polymerization of MAEH in 1 M HCl with VA-044 and ImET at 40 °C.

($Đ_M$ < 1.08) throughout the polymerization of MAEH and no color change was observed indicating improved trithiocarbonate chain-end retention. The pseudo-first-order kinetic plot (Fig. 3a) and the M_n *vs.* conversion plot (Fig. 3c) are both linear as expected. The conversion, molecular weight, and dispersity data for aRAFT polymerization of MAH and MAEH are summarized in Table 1. M_{nexp} values measured for polymerization of MAEH (entries 2a–2c) are in better agreement with $M_{ntheory}$ values, as compared to the greater discrepancy in M_{nexp} and $M_{ntheory}$ values obtained during the aRAFT polymerization of MAH (entries 1a–1c). Collectively, the ASEC, dispersity, and kinetic data agree with the results in the previous section that suggest the CTA is stable during low pH aRAFT polymerization of MAEH.

Retention of active thiocarbonylthio chain ends is crucial for the successful synthesis of block copolymers. To demonstrate high chain end fidelity, a MAEH macro-CTA was synthesized and isolated according to the procedure reported in the ESI† followed by chain-extension with additional MAEH monomer. The ASEC traces of pMAEH before and after chain extension are shown in Fig. 4. The ASEC trace for the macro-CTA is narrow and symmetrical with a molecular weight of 17 600 g mol^{-1} and $Đ_M$ = 1.06. After chain-extension, the ASEC trace shifts to a lower elution volume with a molecular weight of 22 600 g mol^{-1} and $Đ_M$ = 1.04. The ASEC trace of the chain extension remains narrow with no low molecular weight tailing indicating excellent chain extension efficiency and preservation of active trithiocarbonate end groups during purification. This demonstration of ImET-mediated aRAFT polymerization of MAEH is significant, as it is to our knowledge, the first example of successful reversible-deactivation radical polymerization of an unprotected acyl hydrazide-containing monomer and the first example of controlled aqueous RAFT polymerization at pH ≈ 0.

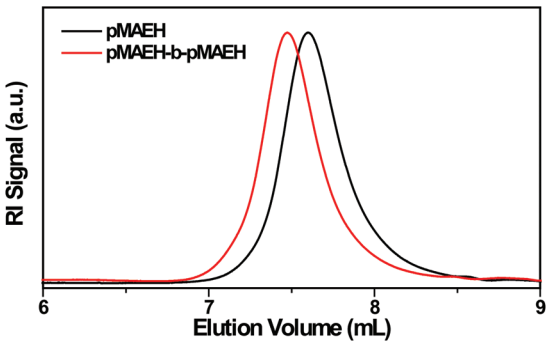

Fig. 4 ASEC traces for pMAEH before (M_n = 17 600 g mol^{-1}, $Đ_M$ = 1.06) (black) and after (M_n = 22 600 g mol^{-1}, $Đ_M$ = 1.04) (red) chain extension.

Conclusions

In summary, the first example of controlled radical polymerization of monomers containing unprotected acyl hydrazide pendent groups was demonstrated using aqueous RAFT polymerization under acidic conditions. This approach eliminates the need for multistep protection/deprotection and post-polymerization procedures to access well-defined acyl hydrazide functionalized polymer scaffolds. A new imidazolium-based trithiocarbonate CTA was synthesized that exhibited

Table 1 Conversion, molecular weight, and dispersity data for the aRAFT polymerization of MAH and MAEH in 1 M HCl at 40 °C [a]

Entry	Monomer	t (m)	Conv[b] (%)	$[M]_0$ (mol L^{-1})	$M_{ntheory}$ (g mol^{-1})	M_{nexp} [c] (g mol^{-1})	$Đ_M$ [c]
1a	MAH	180	24.9	1	8800	15 700	1.25
1b	MAH	360	55.0		19 000	24 100	1.24
1c	MAH	600	71.1		24 600	31 600	1.27
2a	MAEH	180	10.3	1	5600	8900	1.06
2b	MAEH	360	20.2		10 800	13 600	1.05
2c	MAEH	600	38.2		20 100	21 300	1.05

[a] MAH and MAEH were polymerized at 40 °C in 1 M HCl ($[M]_0 : [CTA]_0 : [I]_0$ = 250 : 1 : 0.2 for MAH or $[M]_0 : [CTA]_0 : [I]_0$ = 1 : 0.20 for MAEH) using VA-044 as the initiator. [b] Conversions were determined by ^{1}H NMR spectroscopy. [c] As determined by ASEC-MALLS (0.4% (v/v) TFA and 0.1 M $NaNO_3$ in water).

excellent solubility and stability under acidic conditions and facilitated controlled polymerizations of MAH and MAEH. The low pK_a of the monomers required a pH ≈ 0 (1 M HCl) polymerization medium to sufficiently protonate the hydrazide and avoid degradation of the CTA. The incorporation of an ethyl spacer between the backbone and the acyl hydrazide proved important to avoid intramolecular aminolysis of the trithiocarbonyl end group by the terminal monomer unit. High chain end fidelity was demonstrated *via* chain extension experiments, highlighting the ability to access block copolymer architectures. aRAFT at pH 0 not only enables the facile synthesis of well-defined hydrazide polymer scaffolds, but also provides a vantage point to expand aRAFT polymerization to a broader library of monomers containing low pK_a functional groups.

Acknowledgements

This effort was supported by the National Science Foundation through awards DMR-1056817 and IIA-1430364. EAH and BAA acknowledge support from the NSF Graduate Research Fellowship Program (DGE-1445151).

Notes and references

1 A. Dirksen, S. Dirksen, T. M. Hackeng and P. E. Dawson, *J. Am. Chem. Soc.*, 2006, **128**, 15602–15603.
2 R. J. Wojtecki, M. A. Meador and S. J. Rowan, *Nat. Mater.*, 2011, **10**, 14–27.
3 E. T. Kool, D.-H. Park and P. Crisalli, *J. Am. Chem. Soc.*, 2013, **135**, 17663–17666.
4 X. Su and I. Aprahamian, *Chem. Soc. Rev.*, 2014, **43**, 1963–1981.
5 Y. Iwasaki, H. Maie and K. Akiyoshi, *Biomacromolecules*, 2007, **8**, 3162–3168.
6 T. Etrych, T. Mrkvan, P. Chytil, Č. Koňák, B. Říhová and K. Ulbrich, *J. Appl. Polym. Sci.*, 2008, **109**, 3050–3061.
7 S. Binauld and M. H. Stenzel, *Chem. Commun.*, 2013, **49**, 2082–2102.
8 N. Ballard and S. A. F. Bon, *Polym. Chem.*, 2014, **5**, 6789–6796.
9 D. D. Lane, D. Y. Chiu, F. Y. Su, S. Srinivasan, H. B. Kern, O. W. Press, P. S. Stayton and A. J. Convertine, *Polym. Chem.*, 2015, **6**, 1286–1299.
10 K. Godula and C. R. Bertozzi, *J. Am. Chem. Soc.*, 2010, **132**, 9963–9965.
11 B. S. Murray and D. A. Fulton, *Macromolecules*, 2011, **44**, 7242–7252.
12 M. von Delius, E. M. Geertsema, D. A. Leigh and D.-T. D. Tang, *J. Am. Chem. Soc.*, 2010, **132**, 16134–16145.
13 M. Vetrík, M. Přádný, M. Hrubý and J. Michálek, *Polym. Degrad. Stab.*, 2011, **96**, 756–759.
14 G. Deng, F. Li, H. Yu, F. Liu, C. Liu, W. Sun, H. Jiang and Y. Chen, *ACS Macro Lett.*, 2012, **1**, 275–279.
15 A. Kumar, R. R. Ujjwal, A. Mittal, A. Bansal and U. Ojha, *ACS Appl. Mater. Interfaces*, 2014, **6**, 1855–1865.
16 N. Kuhl, S. Bode, R. K. Bose, J. Vitz, A. Seifert, S. Hoeppener, S. J. Garcia, S. Spange, S. van der Zwaag, M. D. Hager and U. S. Schubert, *Adv. Funct. Mater.*, 2015, **25**, 3295–3301.
17 R. Vartan-Boghossian, B. Dederichs and E. Klesper, *Eur. Polym. J.*, 1986, **22**, 23–36.
18 C. L. McCormick and A. B. Lowe, *Acc. Chem. Res.*, 2004, **37**, 312–325.
19 G. Moad, Y. K. Chong, A. Postma, E. Rizzardo and S. H. Thang, *Polymer*, 2005, **46**, 8458–8468.
20 A. B. Lowe and C. L. McCormick, *Prog. Polym. Sci.*, 2007, **32**, 283–351.
21 M. R. Hill, R. N. Carmean and B. S. Sumerlin, *Macromolecules*, 2015, **48**, 5459–5469.
22 D. B. Thomas, B. S. Sumerlin, A. B. Lowe and C. L. McCormick, *Macromolecules*, 2003, **36**, 1436–1439.
23 J.-F. Baussard, J.-L. Habib-Jiwan, A. Laschewsky, M. Mertoglu and J. Storsberg, *Polymer*, 2004, **45**, 3615–3626.
24 D. B. Thomas, A. J. Convertine, R. D. Hester, A. B. Lowe and C. L. McCormick, *Macromolecules*, 2004, **37**, 1735–1741.
25 Y. Li, B. S. Lokitz and C. L. McCormick, *Angew. Chem., Int. Ed.*, 2006, **118**, 5924–5927.
26 A. W. York, S. E. Kirkland and C. L. McCormick, *Adv. Drug Delivery Rev.*, 2008, **60**, 1018–1036.
27 M. H. Allen, S. T. Hemp, A. E. Smith and T. E. Long, *Macromolecules*, 2012, **45**, 3669–3676.
28 C. J. Ferguson, R. J. Hughes, D. Nguyen, B. T. T. Pham, R. G. Gilbert, A. K. Serelis, C. H. Such and B. S. Hawkett, *Macromolecules*, 2005, **38**, 2191–2204.
29 R. T. A. Mayadunne, E. Rizzardo, J. Chiefari, J. Krstina, G. Moad, A. Postma and S. H. Thang, *Macromolecules*, 2000, **33**, 243–245.
30 J. B. McLeary, F. M. Calitz, J. M. McKenzie, M. P. Tonge, R. D. Sanderson and B. Klumperman, *Macromolecules*, 2005, **38**, 3151–3161.
31 B. A. Abel and C. L. McCormick, *Macromolecules*, 2016, **49**, 465–474.

